PROCEEDINGS of the
23rd International Congress on Acoustics
9 to 13 September 2019 in Aachen, Germany

Acoustic topology optimization of the material distribution on a simply supported plate

Jan VAN DEN WYNGAERT[(1)], Mattias SCHEVENELS[(2)], Edwin REYNDERS[(1)]

[(1)]KU Leuven, Faculty of Engineering Science, Department of Civil Engineering, Kasteelpark Arenberg 40, B-3001 Leuven, Belgium. jan.vandenwyngaert@kuleuven.be, edwin.reynders@kuleuven.be

[(2)]KU Leuven, Faculty of Engineering Science, Department of Architecture, Kasteelpark Arenberg 1, B-3001 Leuven, Belgium. mattias.schevenels@kuleuven.be

Abstract

Lightweight plates typically have a low sound reduction index (SRI) due to their low mass. Their SRI can be increased by roughly 6 dB by doubling the thickness of the plate. The distribution of additional material in a non-uniform way may result in a higher increase in SRI. A good material distribution strategy is therefore needed to reduce the transmitted sound in a certain frequency range. In this paper, the optimal material distribution at a single frequency and in a frequency band for a simple system was considered: a simply supported plate. The SRI is modelled within the hybrid Finite Element-Statistical Energy Analysis (FE-SEA) framework to reduce computational cost while maintaining a high prediction accuracy. The thicknesses of the elements comprising the plate are used as optimization variables. The sensitivity of the SRI to the element thicknesses is derived explicitly because a gradient based optimization algorithm is used. It is observed that the optimization algorithm increases the SRI by shifting the eigenfrequencies of the plate and creating stop bands by locally adding mass that disturbed the mode shapes. In the case of a PMMA-plate, an increase up to 32.1 dB in the SRI is achieved for the single frequency case and up to 29.90 for the frequency band case compared to 6 dB for the uniform material distribution.

Keywords: topology optimization, airborne sound insulation, optimal material distribution, simply supported plate, PMMA plate

1 INTRODUCTION

Lightweight plates typically have a low sound reduction index (SRI) due to their low mass. Following the mass law, an increase of 6 dB can be obtained by doubling the mass of the plate for infinitely large plates under the coincidence frequency. By distributing this added mass onto the plate in a non-uniform way, a higher increase in SRI can be attained.

Up until recently, the prediction of the airborne sound insulation of a simply supported plate had been either too inaccurate or computationally too expensive to allow for numerical design optimization. To model the sound insulation of the plates, the hybrid FE-SEA modelling framework [1, 2] is used. The transmission rooms are modelled to carry a diffuse sound field and are coupled to a finite element model of the plate to reduce the computational cost while retaining a high prediction accuracy.

In this paper, the optimal material distribution for a maximal sound insulation is considered. The sound insulation at a single frequency or the minimum of the sound insulation in a certain frequency band are used as objective functions. A volume constraint is used to limit the total material used. The optimization problem is solved using the standard Optimality Criteria method [3].

The rest of this paper is structured as follows: in Section 2 the prediction of the transmission loss of a simply supported plate is elaborated. The optimization problem is formulated in Section 3. The results of the optimization are shown in Section 4 and discussed in Section 5. Some conclusions and final remarks are given in Section 6.

2 Transmission loss prediction

The plate is modelled deterministically to capture its vibration behavior in full detail while the sound fields in the sending and receiving rooms are modelled as diffuse. The hybrid FE-SEA modelling framework [1, 2] is used to rigorously couple the diffuse sound fields in the transmission rooms to the deterministic wall model by employing the diffuse field reciprocity relationship [4]. In what follows, the deterministic model of the wall system is explained first. Subsequently, the interaction between the wall and the sound fields in the adjoining rooms is described.

2.1 Plate model

The plate is a polymethyl methacrylate (PMMA) panel with density ρ = 1275 kg/m^3, modulus of elasticity E = 4.5 GPa, Poisson's ratio v = 0.35, a minimal thickness of 15 mm and dimensions 1x1 m^2. In the present work, the plate is modeled numerically, using the finite element method [5]. As the plate thickness is small compared to its lateral dimensions, it can be adequately modelled with structural shell elements. The particular element type that is employed here is a four node DKT element with six degrees of freedom – three displacements and three rotations – at each node. Simply supported boundary conditions are assumed.

The model is then employed for computing the natural frequencies and mass-normalized displacement mode shapes of the simply supported plate. These numerically computed mode shapes are taken to be basis functions for the computation of the transmission loss. The corresponding generalized coordinates are then the modal amplitudes of the plate. The equation of motion of the plate therefore reads

$$\mathbf{D}_{\mathrm{pl}}\mathbf{q}_{\mathrm{pl}} = \tilde{\mathbf{f}}_{\mathrm{pl}}, \tag{1}$$

where $\mathbf{D}_{\mathrm{pl}}$ is a diagonal matrix with entries

$$\mathrm{D}_{\mathrm{pl},kk} = -\omega^2 + \omega_{\mathrm{pl},k}^2(1 + i\eta_{\mathrm{pl},k}), \tag{2}$$

with $\omega_{\mathrm{pl},k}$ the numerically computed angular natural frequency of mode k the plate, with corresponding mode shape $\phi_{\mathrm{pl},k}$, and $\eta_{\mathrm{pl},k}$ the corresponding structural damping loss factor.

2.2 Transmission room model

Within the hybrid DET-SEA framework, a transmission suite (room-wall-room) model has been developed by Reynders et al. [2, 6, 7]. In this model, which is adopted also in the present work, the rooms are taken to carry a diffuse field, while the wall is modeled deterministically. The hybrid model contains two diffuse (SEA) subsystems - the sending and receiving rooms - and, in the context of a sound transmission analysis, the quantity of interest is the so-called coupling loss factor, η_{12}, between both rooms. Although the coupling loss factor is a random quantity (because the sound fields in the rooms are random, diffuse fields), only its mean value will be of interest in the present analysis as the intention is to predict the mean sound insulation of the wall across the ensemble of random sound fields. The coupling loss factor relates directly to the sound transmission coefficient, τ, which is defined as the ratio between the power flow from room 1 to room 2 through the wall, and the incident sound power on the wall in room 1. The relationship at frequency ω reads [8]

$$\tau = \frac{4V_1\omega}{\mathrm{L_x L_y} c}\eta_{12}, \tag{3}$$

where V_1 denotes the volume of the sending room, $\mathrm{L_x}$ and $\mathrm{L_y}$ are the width and the height of the wall and c is the speed of sound in air. The sound insulation of the wall then immediately follows from

$$\mathrm{R} := 10\log\frac{1}{\tau} = 10\log\frac{\mathrm{L_x L_y c}}{4\mathrm{V_1}\omega\eta_{12}}. \tag{4}$$

The mean value of the coupling loss factor is obtained from [1]

$$\eta_{12} = \frac{2}{\pi \omega n_1} \sum_{r,s} \mathrm{Im}\left(\mathbf{D}'_{\mathrm{dir2}}\right)_{rs} \left(\mathbf{D}_{\mathrm{tot}}^{-1} \mathrm{Im}\left(\mathbf{D}'_{\mathrm{dir1}}\right) \mathbf{D}_{\mathrm{tot}}^{-\mathrm{H}}\right)_{rs} \tag{5}$$

where

$$\mathbf{D}_{\mathrm{tot}} := \mathbf{D}_{\mathrm{pl}} + \mathbf{D}'_{\mathrm{dir1}} + \mathbf{D}'_{\mathrm{dir2}}. \tag{6}$$

$\mathbf{D}'_{\mathrm{dir1}}$ and $\mathbf{D}'_{\mathrm{dir2}}$ are the direct field acoustic dynamic stiffness matrices expressed in terms of the generalized wall coordinate vector $\mathbf{q}_{\mathrm{pl}}$, and n_1 is the modal density in the first transmission room.

The direct field response of a room is the sound field that would occur if the room would be of infinite extent, in other words, if the room would behave as an acoustic half-space as seen from the room-wall interface when that interface is embedded in an infinite planar baffle. The related acoustic dynamic stiffness matrix is then termed the direct field dynamic stiffness matrix $\mathbf{D}_{\mathrm{dir}}$ of the room. For room 1 for example, the direct field dynamic stiffness matrix $\mathbf{D}_{\mathrm{dir1}}$ describes the relationship between the displacements and forces at the interface with the plate:

$$\mathbf{D}'_{\mathrm{dir1}} \mathbf{q}_{\ell 1} = \tilde{\mathbf{f}}_{\mathrm{dir1}}. \tag{7}$$

where the components of $\tilde{\mathbf{f}}_{\mathrm{dir1}}$ denote the forces acting on the (generalized) degrees of freedom of the plate $\mathbf{q}_{\ell 1}$ due to the pressure field in the acoustic half-space.

3 Optimization methodology

The sound insulation of a plate, computed according to (4), is a property that depends on the frequency, the plate setup and the rooms separated by the element. The airborne sound insulation is modelled in laboratory conditions that comply with the ISO 10140-2:2010 standard [9]. This standard defines among others the volume of the transmission rooms and the size of the plate section. In this paper the volume and measurement opening of the KU Leuven Laboratory of Acoustics are considered.

3.1 Parametrization

In this paper, the plate thickness of a simply supported PMMA plate is optimized for an optimal airborne sound insulation. The PMMA-plate is divided into shell elements using a square grid. The individual element thicknesses, $\mathbf{x}$, are used as design variables.

3.2 Optimization problem and constraints

The sound insulation can be evaluated at a single number frequency of in a frequency band. When the sound insulation is evaluated in a frequency band either the sum of the individual sound insulations can be optimized or the minimum sound insulation in the frequency band can be maximized. In this paper, the minimum sound insulation is optimized in the case of a frequency band.

$$\begin{aligned} \max_{\mathbf{x}} \quad & \min(\mathrm{R}(\mathbf{x}, \mathrm{f}), \mathrm{f} \in \mathrm{D}) \\ \text{s.t.} \quad & \sum_i \mathrm{x}_i \mathrm{A}_i \leq 2 \mathrm{A}_{\mathrm{tot}} \mathrm{t}_{\mathrm{min}} \\ & \mathrm{t}_{\mathrm{min}} \leq \mathrm{x}_i \leq 4 \mathrm{t}_{\mathrm{min}} \end{aligned} \tag{8}$$

with $\mathrm{A}_{\mathrm{tot}}$ the total surface area of the plate and D the frequency band of interest.

The sound insulation of the simply supported plate is optimized under a volume constraint. The minimal thickness of the simply supported plate is $\mathrm{t}_{\mathrm{min}} = 15\,\mathrm{mm}$ and ensures there is always a minimum amount of material between the transmission rooms. The total volume of the plate cannot exceed the volume of a plate with homogeneous thickness $2\mathrm{t}_{\mathrm{min}}$. The maximal thickness of the plate cannot exceed $4\mathrm{t}_{\mathrm{min}}$, as shown in Eq. (8).

Table 1. Comparison of the Sound Reduction Index (SRI) shows an increase up to 29.9 dB in the case of a frequency band and 32.1 dB for a single frequency with respect to the reference plate.

Case	Frequency (band) [Hz]	Reference SRI [dB]	Optimized SRI [dB]
1	53	0.00	32.12
2	134	16.03	45.90
3	210	33.28	45.67
4	50-100	0.00	29.90
5	100-150	15.90	34.05
6	50-300	0.00	17.35

The optimization problem is solved using the standard Optimality Criteria method [3]. As a starting point of the optimization, a plate with a uniform thickness of $2t_{\min}$ is used. The optimization is performed on a 21x21 grid.

In what follows, six setups are considered: the optimization of the sound insulation at a single frequency being either the first, second or third eigenfrequency of the plate with a uniform thickness $2t_{\min}$, and the optimization in a frequency band of 50-100 Hz, 100-150 Hz and 50-300 Hz.

3.3 Sensitivity analysis

By direct analytical derivation, it can be shown that, after some algebra, the sensitivity of the coupling loss factor can be written as

$$\frac{\partial \eta_{12}}{\partial \mathrm{x}_i} = \frac{4}{\pi \omega n_1}\left[\mathrm{Re}\left(\sum_{rs}(-\mathbf{D}_{\mathrm{tot}}^{-T}\mathbf{A}\mathbf{C}^{\mathrm{T}})_{rs}\left(\frac{\partial \mathbf{D}_{\mathrm{tot}}}{\partial \mathrm{x}_i}\right)_{rs}\right) + 2\,\mathrm{Im}\left(\sum_{rs}(\mathbf{E}\,\mathrm{Re}(\mathbf{C}))_{rs}\left(\frac{\partial \phi}{\partial \mathrm{x}_i}\right)_{rs}\right)\right], \tag{9}$$

with

$$\mathbf{A} := \mathrm{Im}\left(\mathbf{D}'_{\mathrm{dir2}}\right),\ \mathbf{C} := \mathbf{D}_{\mathrm{tot}}^{-1}\mathrm{Im}\left(\mathbf{D}'_{\mathrm{dir1}}\right)\mathbf{D}_{\mathrm{tot}}^{-\mathrm{H}} \text{ and } \mathbf{E} := \mathbf{D}_{\mathrm{dir2}}\phi_{\mathrm{pl}}. \tag{10}$$

with $\mathbf{D}_{\mathrm{dir2}}$ the direct field dynamic stiffness matrix in room 2 in terms of the physical degrees of freedom of the plate.

The derivative of the total dynamic stiffness matrix can be elaborated as:

$$\frac{\partial \mathbf{D}_{\mathrm{tot}}}{\partial \mathrm{x}_i} = \frac{\partial \mathbf{D}_{\mathrm{pl}}}{\partial \mathrm{x}_i} + \frac{\partial \mathbf{D}'_{\mathrm{dir1}}}{\partial \mathrm{x}_i} + \frac{\partial \mathbf{D}'_{\mathrm{dir2}}}{\partial \mathrm{x}_i} \tag{11}$$

$$= \frac{\partial \mathbf{D}_{\mathrm{pl}}}{\partial \mathrm{x}_i} + 2\frac{\partial \phi_{\mathrm{pl}}^{\mathrm{T}}}{\partial \mathrm{x}_i}\mathbf{D}_{\mathrm{dir1}}\phi_{\mathrm{pl}} + 2\phi_{\mathrm{pl}}^{\mathrm{T}}\mathbf{D}_{\mathrm{dir1}}\frac{\partial \phi_{\mathrm{pl}}}{\partial \mathrm{x}_i}, \tag{12}$$

with

$$\frac{\partial \mathrm{D}_{\mathrm{pl},kk}}{\partial \mathrm{x}_i} = 2\omega_{\mathrm{pl},k}(1 + i\eta_{\mathrm{pl},k})\frac{\partial \omega_{\mathrm{pl},k}}{\partial \mathrm{x}_i}. \tag{13}$$

The gradients of the angular natural frequencies and mode shapes are computed according to [10].

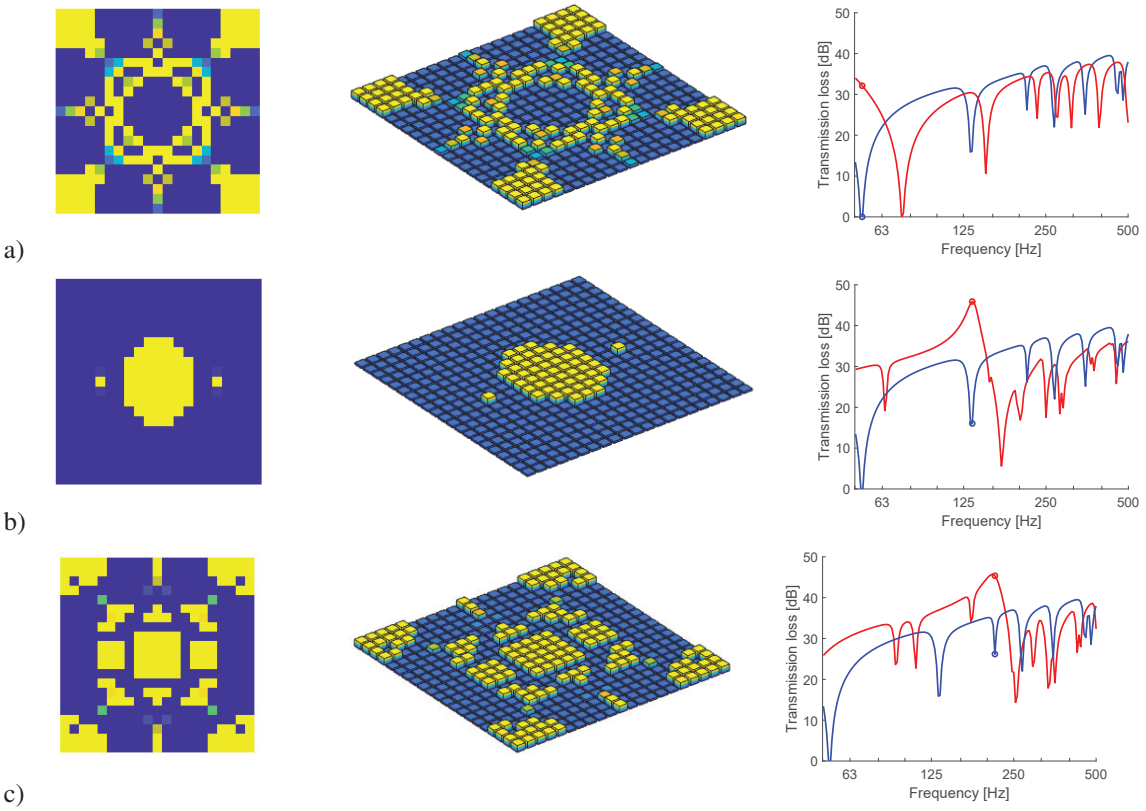

Figure 1. Thickness and sound insulation curve of of the plate optimized at a) 53, b) 132 Hz and c) 210 Hz. The sound insulation of the optimized plate is shown in red and the sound insulation of the reference plate is shown in blue. The frequency at which the optimization is performed is indicated with a dot.

4 Results

The sound insulation of the optimized plates is compared to a reference case where the plate has a uniform thickness of $2t_{min}$, which is the maximal mass that still satisfies the volume constraint. The sound insulation is respectively given in blue for the reference case and in red for the optimized plates in Figs. 1-2.

5 Discussion

In the first case, the sound insulation is optimized at 53.5 Hz. This single frequency corresponds to the first eigenfrequency of the plate in the reference case. The optimized shape, shown in Fig. 1.a, exhibits stiffening in the corners and the middle of the plate. This increases the first eigenfrequency, resulting in a stiffness controlled zone.

For the second case, the sound insulation is optimized at the second and third eigenfrequency of the reference plate at 134 Hz in the reference case. The optimized shape, shown in Fig. 1.b, displays a single centralized mass. This results in an antiresonance at 134 Hz.

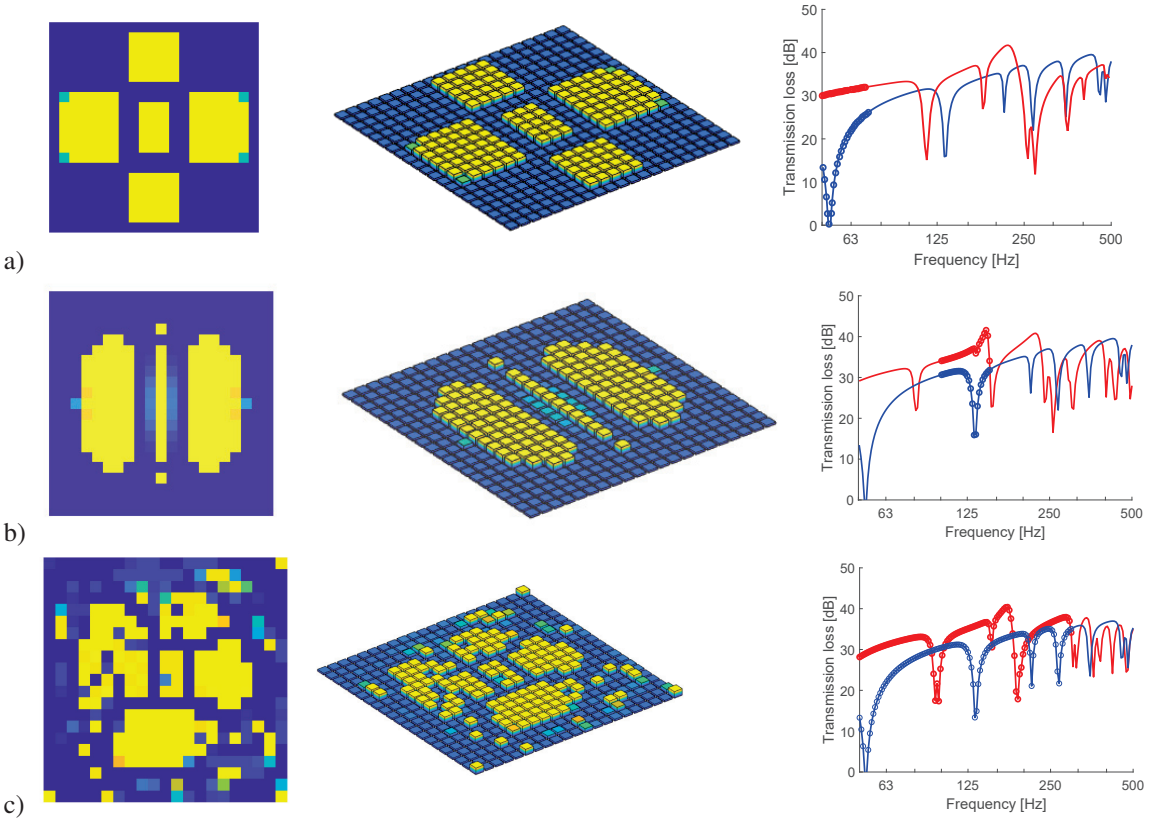

Figure 2. Thickness and sound insulation curve of of the plate optimized in a frequency band of a) 50-100 Hz, b) 100-150 Hz and c) 50-300 Hz. The sound insulation of the optimized plate is shown in red and the sound insulation of the reference plate is shown in blue. The frequencies at which the optimization is performed are indicated with a dot.

In the third case, the sound insulation is optimized at the fourth eigenfrequency of the reference plate which corresponds to the 2-2-mode in the reference case. The optimized shape, shown in Fig. 1.c. The eigenfrequency of the 2-2-mode of the optimized plate is shifted from 210 to 174 Hz. This results in an antiresonance at 210 Hz.

In the fourth case, the sound insulation is optimized in the frequency range of 50-100 Hz which comprises only the first mode in the reference case. The minimum of the sound insulation in this band is maximized. The optimized shape, shown in Fig. 2.a, shows four regions where the material is arranged around a central part. The two horizontal gaps between the bottom, three middle and top masses, and the two vertical gaps between the left, three middle and right masses result in a low plate bending stiffness in both directions. This results in a first eigenfrequency of 26.4 Hz. The second and third eigenfrequencies, at respectively 117.4 and 117.6 Hz, stay relatively close to the original eigenfrequencies of the homogeneous plate and out of the frequency band of interest. This results in a stop band between 27 and 117 Hz with a high sound insulation.

In the fifth case, the sound insulation is optimized in the frequency range of 100-150 Hz, comprising two coincident modes in the reference case. The minimum of the sound insulation in this band is maximized. The optimized shape, shown in Fig. 2.b, shows two regions of concentrated material and a central line. By shaping the added material as ellipses, the eigenfrequencies of the 2-1- and 1-2-bending mode of the plate no longer coincide since the bending stiffness in the two orthogonal directions is different. The large dip in the sound

insulation at 132 Hz for the homogeneous plate, shown in Fig. 2.b, gets shifted to 170 Hz. This dip corresponds to the 2-1-bending mode of the plate. The eigenfrequency of the 1-2-mode of the plate is shifted to 100 Hz. This optimal shape also shows good results in the 50-100 Hz range since the first eigenfrequency is also shifted to the low frequency range, though the sound insulation is lower than the optimal distribution of the first case.

In the sixth case, the sound insulation is optimized in the frequency range of 50-300 Hz, comprising six modes in the reference case, of which two are coincident modes. The minimum of the sound insulation in this band is maximized. The optimized shape, shown in Fig. 2.c, shows an irregular distribution of the material. The first mode is shifted down out of the relevant frequency range. The eigenfrequencies of the 2-1- and 1-2-bending mode of the plate no longer coincide since the bending stiffness in the two orthogonal directions is different. This results in a dip in the sound insulation that is less shallow compared to the reference case. The irregular pattern also disturbs the 2-2-bending mode resulting in only a small dip in the sound insulation at 153 Hz.

6 Conclusions

In this paper, the airborne sound insulation of a simply supported plate is maximized by optimizing the plate thickness under a maximal material constraint. The sound insulation of the plate is modelled in the hybrid FE-SEA framework to lower the computational cost while retaining a high accuracy.

By shaping the added material to either increase or decrease the plate bending stiffness in different ways to shift modes or split up coinciding modes, the sound insulation is effectively maximized.The sound insulation shows an increase up to 32.1 dB for the single frequency optimization and 29.9 dB for the frequency band optimization.

Acknowledgments The research presented in this paper has been performed within the framework of the research project G0A7717N AcOpt: Numerical optimization of the airborne sound insulation of single and double walls, funded by the Research Foundation - Flanders (FWO), Belgium, and the research project ERC-2016-STG: Virtual building acoustics: a robust and efficient analysis and optimization framework for noise transmission reduction, funded by the European Research Council (ERC). The financial support by FWO and ERC is gratefully acknowledged.

References

[1] P.J. Shorter and R.S. Langley. Vibro-acoustic analysis of complex systems. *Journal of Sound and Vibration*, 288(3):669–699, 2005.

[2] E. Reynders, R.S. Langley, A. Dijckmans, and G. Vermeir. A hybrid finite element - statistical energy analysis approach to robust sound transmission modelling. *Journal of Sound and Vibration*, 333(19):4621–4636, 2014.

[3] M. P. Bendsøe and O. Sigmund. *Optimization of structural topology, shape, and material*, volume 414. Springer, 1995.

[4] P.J. Shorter and R.S. Langley. On the reciprocity relationship between direct field radiation and diffuse reverberant loading. *Journal of the Acoustical Society of America*, 117(1):85–95, 2005.

[5] K.J. Bathe. *Finite Element Procedures*. Prentice-Hall, Englewood Cliffs, NJ, second edition, 1996.

[6] C. Decraene, A. Dijckmans, and E.P.B. Reynders. Fast mean and variance computation of the diffuse sound transmission through finite-sized thick and layered wall and floor systems. *Journal of Sound and Vibration*, 422:131–145, 2018.

[7] E. Reynders, C. Van hoorickx, and A. Dijckmans. Sound transmission through finite rib-stiffened and orthotropic plates. *Acta Acustica united with Acustica*, 102(6):999–1010, 2016.

[8] M.J. Crocker and A.J. Price. Sound transmission using statistical energy analysis. *Journal of Sound and Vibration*, 9(3):469–486, 1969.

[9] International Organization for Standardization. *ISO 10140-2: Acoustics – Laboratory measurement of sound insulation of building elements – Part 2: Measurement of airborne sound insulation*, 2010.

[10] Siddhi Vijendra. *A generalized approach for calculation of the eigenvector sensitivity for various eigenvector normalizations*. PhD thesis, University of Missouri – Columbia, 2005.